We formulate assumptions making it possible to obtain the results given above: $u_\infty/c_0 \ll 1$ is smallness of the correction for compressibility, applicability of an acoustic approximation, $\mu/(\rho_0 u_\infty d) \ll 1$ is smallness of the viscosity contribution, $Y_0/(\rho_0 u_\infty^2) \ll 1$ is smallness of the correction due to strength. The assumption $Y_0/g \ll 1$ is immaterial, and it makes it possible to simplify the form of the final equations.

The approach developed for calculating corrections for the first approximation permits apparent generalization in the case of impact of jets with different strength properties since flow for the zero approximation does not depend on rheology of the jet materials.

LITERATURE CITED

1. M. Van Dyke, Perturbation Methods in Fluid Mechanics, Academic Press, New York (1964).
2. M. A. Lavrent'ev and B. V. Shabat, Methods of Complex Displacement Function Theory [in Russian], Nauka, Moscow (1973).
3. P. H. Pidsley, "A numerical study of long rod impact into a large target," J. Mech. Phys. Solids, 32, No. 4 (1984).
4. B. S. Hangstad and O. S. Dulum, "Finite compressibility in shaped charge jet and long rod penetration — the effect of shocks," J. Appl. Phys., 52, No. 8 (1981).

EXPERIMENTAL STUDY OF VISCOUS INSTABILITY IN A POROUS MEDIUM

O. B. Bocharov, O. V. Vitovskii, Yu. P. Kolmogorov, and V. V. Kuznetsov

UDC 532.546

Viscous instability of the displacement front in a porous medium arises when a liquid with a higher viscosity is displaced by a less-viscous liquid or gas. A large number of theoretical and experimental studies have been made of the formation and development of the fingers of displacing liquid that are produced in the process (see the reviews in [1, 2]). The displacement stability condition for neutrally wetted porous media was first obtained in [3]. The flow of liquids in this case occurs in different regions (piston displacement) and the capillary forces are taken into account in the boundary conditions at the displacement front. The nonlinear stage of development of liquid instability in the case of piston displacement was studied experimentally and theoretically in a Hele–Shaw cell [4].

When a porous medium is wetted well by one of the liquids, the two liquids flow jointly in porous space throughout the entire displacement region [5]. The condition for the stability of the displacement front against small perturbations with allowance for two-phase flow was given in [6]. Elsewhere [7] we showed that, in the case of unstable displacement capillary forces, which cause return flows of liquid in regions of high saturation gradients of the displacing liquid, stabilize the length of the fingers. At the same time, experimental data on the structure and growth dynamics of fingers of the displacing liquid in a porous medium during developed two-phase flow are lacking at present.

In this communication we report the results of an experimental study of the distinctive features in the development of fingers of displacing liquid during unstable displacement under the conditions of developed two-phase flow in the displacement region. The experimental data obtained on the structure and growth dynamics of fingers are compared directly with the results of numerical calculations on the basis of the Masket–Leverett model.

The experiments were carried out on a rectangular model of a porous medium with a working part measuring $1 \times 20 \times 60$ cm, arranged horizontally. The working part was filled with quartz sand, which was then vibrocompacted with the porous state completely saturated with water. This made it possible to obtain a homogeneous porous medium with permeability ~10 μm^2 and porosity $m = 0.4$. After the vibrocompaction, the porous medium was dried, vacuum

Novosibirsk. Translated from Zhurnal Prikladnoi Mekhaniki i Tekhnicheskoi Fiziki, No. 4, pp. 79-84, July-August, 1989. Original article submitted December 15, 1987; revision submitted April 7, 1988.

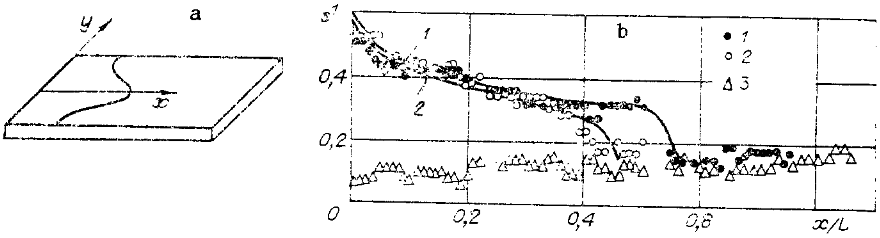

Fig. 1

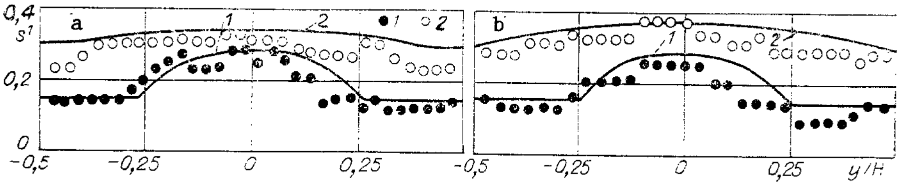

Fig. 2

evaporated and saturated with a 1 g/liter NaCl aqueous solution, which made it possible to sustain uniform wettability of the porous medium with water during the experiments. A sample of the porous medium was filled with liquid possessing an enhanced viscosity of 1.2 to 80 mPa·sec. Two types of experiments were carried out. In the first, the displacing liquid wetted the porous medium well. A 1 g/liter NaCl aqueous solution was used as the displacing liquid and hydrocarbon liquids with different viscosities were used as the displaced liquid. When the effective part was filled with a hydrocarbon liquid before the experiment, part of the water continued to be entrapped by the capillary forces; this simulated the initial saturation of the displacing liquid that is characteristic, e.g., of oil strata under natural conditions. In the second type of experiment, the displacing liquid did not wet the porous medium. As the displacing liquid we used refined kerosene with μ = 1.2 mPa·sec and as the displaced liquid we used water—glycerine solutions with μ = 4-20 mPa·sec. In order to simulate the initial saturation of the liquid, the aqueous solution of NaCl initially filling the porous medium was displaced by kerosene, which was then displaced by water—glycerine solution before the experiment. This made it possible to preserve the preferred wettability of the porous medium by the water—glycerine solution, which was used as the displacing liquid with increased viscosity.

All the experiments were carried out with a constant flow rate of displacing liquid, delivered to the entrance chamber of the working part. The pressure field at the entry into the porous medium was equalized in this chamber. The phase permeabilities for the indicated types of experiment were determined at low displacement rates under steady-state conditions. The capillary pressure curves were measured by the semiimpermeable baffle method.

The displacement process is nearly two-dimensional when the thickness of the working part is small (1 cm) in comparison with its width (20 cm). The saturation field of the displacing liquid was measured with γ-ray tracers. A radioactive substance Promeran, containing a mercury isotope, was introduced into the aqueous phase. The spatial distribution of the γ rays during the experiments was measured with a SEGAMS (Hungary) gamma chamber, in which an Na/I scintillation crystal with a diameter of 0.3 m is the measuring element. A standard high-resolution collimator gave the measuring system a 5 × 5 mm area resolution and a 14% energy resolution in the system. The computer processing the image made allowance for the fact that the sensitivity of the detector photomultiplier is nonuniform and that the γ rays are random.

Figures 1 and 2 show the profiles of the saturation s^1 of the displacing liquid in the longitudinal and transverse sections, respectively, of a sample of the porous medium under conditions of unstable displacement, when fingers of displacing liquid are formed. The displacing liquid does not wet the porous medium. The profiles of the saturation s^1 were obtained with a displacing-liquid filtration rate $v_0 = 3.33 \cdot 10^{-5}$ m/sec at the inlet, absolute permeability of the porous medium $k = 12\ \mu m^2$, porosity $m = 0.41$, interphase tension $\sigma = 30$ mN/m, boundary inflow angle of displacing liquid on a smooth quartz plate 180°, boundary outflow angle 160°, viscosity of displaced liquid $\mu_2 = 20$ mPa·sec, and viscosity ratio of the displacing and displaced liquids $\mu_0 = \mu_1/\mu_2 = 0.59$. The longitudinal saturation profiles (Fig.

1b) were obtained at time $\tau = 0.5$ (dimensionless time defined as $\tau = tv_0/mH$, where t is the time and H is the width of the model); points 1 were obtained in the central longitudinal cross section $y/H = 0$, points 2 in the side longitudinal section $y/H = 0.4$, and points 3 correspond to the initial saturation s_0^1 of the displacing liquid up until displacement begins in section $y/H = 0$ and practically coincide with it in section $y/H = 0.4$. The coordinate system is shown in Fig. 1a.

An important feature of the displacement process in a porous media is that, in contrast to the Hele–Shaw cell, displacement is not of the piston type. Corresponding to the displacement front in Fig. 1b is a region of abrupt change in saturation in the head part and a smoother change in the tail part of a growing finger (points 1 and 2). Behind the displacement front the two liquids flow together, with the saturation of the displacing liquid increasing gradually. As follows from analysis of the solutions of displacement problems using the Masket–Leverett model, the displacement front has a finite length, which is determined by capillary return flows of liquids in regions of large saturation gradients [5]. At low values of the parameter $\varepsilon = \sigma\sqrt{km}/(v_0\mu_2L)$ (L is the length of the model) the saturation of the displacing liquid at the displacement front can be estimated from the solution of the Buckley–Leverett problem, i.e., without allowance for the capillary forces [5]. For phase permeabilities corresponding to the displacement in Fig. 1b, the front saturation in the Buckley–Leverett solution is $s_c^1 = 0.31$, which is close to the saturation value observed in experiments in regions of small saturation gradients behind the saturation front in the head part of the growing finger. The ratio of the mobilities of the two-phase filtration flow behind and ahead of the displacement front for the experimental data of Figs. 1 and 2 is 1.6 and, according to the criterion of [7], the displacement can be unstable.

The advanced development of the displacement front in section $y/H = 0$ in comparison with section $y/H = 0.4$ testifies to the deformation of the displacement front and the formation of a tongue of displacing liquid. The saturation profiles of the displacing liquid in transverse section $x/L = 0.3$ of a sample of the porous medium (see Fig. 2a) at $\tau = 0.295$ and 0.5 (points 1 and 2) and analysis of the isolines of the constant saturation of the displacing liquid (isosat curves) show that during displacement there is preferential development of displacement-front perturbations with wavelength equal to the width of the model (see Fig. 1a). The finger formed with width equal to half the width of the sample does not have a smooth shape and contains displacement-front perturbations with shorter wavelengths (see Fig. 2a, $\tau = 0.295$). The experiments carried out showed that the largest deformation of isosat curves is observed for near-front saturations in the head part of the finger ($s^1 \approx 0.3$). For high saturations, this corresponds to large distances from the displacement front, the deformation of the isosat curves decreases, and for $s^1 > 0.4$ and manifests itself only slightly (see Fig. 2a, $\tau = 0.5$).

In the experiments the flow rate of the displacing liquid was uniform over the cross section of the working part. Small perturbations of the displacement front, whose development leads to the formation of a finger, evidently arise because of microinhomogeneities of the permeability field of the quartz sand. The fact that the displacement front was stable when the displacing and displaced liquids had similar viscosities showed that the nonuniformity of the permeability field is small.

The number of fingers does not increase as the displacement velocity increases to $v_0 = 7\cdot10^{-5}$ m/sec (see Fig. 2b). The transverse saturation profiles of the displacing liquid are shown in Fig. 2b for the section $x/L = 0.26$ at time $\tau = 0.255$ and 0.5 (points 1 and 2). As in the case with $v_0 = 3.33\cdot10^{-5}$ m/sec, we observed preferential development of one finger with a width equal to nearly half the width of the sample of the porous medium. The experimental data on the finger length $\ell_f^* = \ell_f/H$ as a function of time for $v_0 = 7\cdot10^{-5}$, $3.33\cdot10^{-5}$, and $1.4\cdot10^{-6}$ m/sec (points 1, 2, and 4) are shown in Fig. 3 (points 3 represent the time dependence of the doubled amplitude of perturbations of the isosatic curves with $s^1 = 0.4$). At low displacement velocities the displacement front is stable even when the ratio of the liquid viscosities is small, $\mu_0 = 0.059$ (points 4 in Fig. 3).

When the porous medium can be wetted well by one of the liquids, the displacement is characterized by a well-developed two-phase flow in the entire displacement region. The displacement front in this case includes the region of two-phase flow in which there exist large, but finite, saturation gradients of the displacing liquid (see Figs. 1 and 2). To generalize the experimental data on unstable displacement in the nonlinear stage of finger development, we carried out calculations on unstable displacement within the framework of

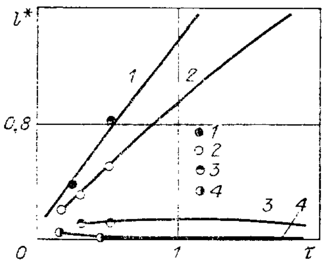

Fig. 3

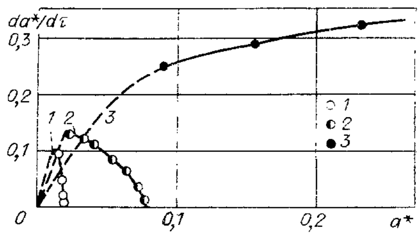

Fig. 4

the Masket–Leverett equations of two-phase filtration with allowance for the capillary forces. The computational method was described in [7]. The computations were performed by the IMPES technique using the conservative difference scheme in a two-dimensional region with parameters corresponding to the conditions of the experiments. The relative phase permeabilities were determined in the experiments on stable displacement and under the conditions of the experiments of Figs. 1 and 2 they have the form

$$k_1(s) = 0.305s^{2.3} + 0.31s^{1.9},\ k_2(s) = (1 + 20s)^{0.125}[0.12(1 - s)^{1.6} + 0.35(1 - s)^{3.6}],$$

where $s = (s^1 - s_0{}^1)/(s_*{}^1 - s_0{}^1)$ is the normalized saturation; $s_*{}^1$ is the limiting value of saturation of the displacing liquid. The Leverett function was found from the capillary pressure curve $J(s) = -0.226(s + 0.01)^{0.25}[1 + (s + 0.119)^3]$.

Since we are considering the nonlinear stage of fingering (the length of the finger is comparable with its width), in the computational modeling the initial shape of the fingers was prescribed by a nonuniform water flow rate over the section at $x/L = 0$ at the initial time $\tau \leq \tau_0$: $v(0, y, \tau) = v_0(1 - \alpha\cos 2\pi y)$. The value of α was chosen so that at $x/L = 0.09$, i.e., small distances from the inlet, the finger length ℓ_f would coincide with the experimentally observed length. The boundary conditions corresponding to the conditions of the experiments (constant water flow rate over the section at $x/L = 0$) were maintained at $\tau > \tau_0$ and the difference in the fingers was studied.

The rates of change in the amplitude of the displacement-front perturbations calculated as a function of the amplitude $a^* = a/H$ ($a = \ell_f/2$), are given in Fig. 4 (points 1-3 are for perturbations with wavelength $\lambda/H = 0.2$, 0.3, and 1). The calculations were carried out in a rectangular region of width $H = 10\lambda_c$, where λ_c is the critical wavelength, which was defined in [7] as $\lambda_c = 2\pi\sigma\sqrt{km}\Phi_c(M_c + 1)/\mu_2 v_0 F_c(M_c - 1)$, $\Phi_c = \int^{s_c} k_2(s)F(s)(dJ/ds)ds$, $F_c = k_1(s_c)/[k_1(s_c) + \mu_0 k_2(s_c)]$, and $M_c = [k_1(s_c)\mu_0{}^{-1} + k_2(s_c)]/k_2(0)$ is the ratio of mobilities at the displacement front.

At $\lambda \leq \lambda_c$ the capillary diffusion in the zone of large saturation gradients of the displacing liquid in the neighborhood of the displacement front is stabilized by the viscosity instability and small perturbations do not develop. Perturbations with $\lambda_m = 2\lambda_c$ occur in the region of small amplitudes of maximum growth rate [7], line 1 in Fig. 4. The growth rate decreases with increasing wavelength, lines 2 and 3 for $\lambda/\lambda_c = 3$ and 10. In the nonlinear stage of development of perturbations for $\lambda/\lambda_c = 2$ (points 1 in Fig. 4) at $a^* = 0.018$ the finger length stabilizes, as pointed out in [6]. This is because the capillary return flow of displacing flow from the head to the tail of the growing finger increases as the curvature of the finger increases with its amplitude. As the wavelength increases, the limiting length of the finger and the rate of change of its amplitude grow [7] and at $\lambda/\lambda_c = 10$ in the range of amplitudes $a^* < 0.3$, amplitude stabilization is not observed while the rate of change in amplitude with time is maximum (points 3 in Fig. 4). Thus, in the nonlinear stage of perturbation development, perturbations with wavelength equal to the width of the displacement region is developed preferentially. The existence of perturbations with shorter wavelengths results in distortion of the shape of the growing finger, which is seen from the experimental saturation profiles in Fig. 2a, b.

The experimental data on the structure and growth dynamics of fingers with the results of calculations on the basis of the Masket–Leverett model, which were carried out for $\lambda = H$, are compared in Figs. 1-3. The results of the calculations are represented by curves, whose numbers correspond to the numbers of the experimental points with which the comparison is made. The anomalies of finger growth in the initial part of the porous medium, when they are small, were not taken into account, since analysis of the curves of Fig. 4 indicates that, under the conditions of the experiments ($H/L = 0.3$), the growth of perturbations with the wavelength of maximum growth λ_m ceases at $x/L = 0.03$ and their amplitude does not exceed $a/L = 0.015$. As a result of the development of long-wavelength perturbations, one finger with $\lambda = H$ is formed at $x/L = 0.09$. In view of this, in numerical computations using the Masket–Leverett model a perturbation with $\lambda = H$ was formed with the same amplitude at $x/L = 0.09$ as the experimental amplitude. The boundary conditions corresponding to the experimental conditions (constant displacing-liquid flow rate over the section at $x/L = 0$) were then maintained. On the whole, in the entire displacement region good agreement is observed between the results of the computations and the experimental data, both in regard to the internal structure of the displacement region (Figs. 1 and 2) and in regard to the finger length as a function of time (Fig. 3). The calculated curves 1-4 in Fig. 3 correspond to H/λ_c = 19.3, 9.2, 9.2, and 0.4. At $H/\lambda_c = 0.4$ perturbations were not found to grow in either the computations or the experiments.

The experiments also studied the stability of the displacement front when the porous medium was wetted well by the displacing liquid (boundary angle of inflow on a smooth quartz plate $\theta \approx 20°$, angle of outflow ~0). The experiments showed that at displacement velocities $v_0 < 10^{-4}$ m/sec the displacement front is stable in the entire range of viscosity ratios studied, $0.013 < \mu_0 < 0.8$. Computations using the phase permeabilities and the capillary pressure, obtained for this type of experiments, showed that in all the experiments $H/\lambda_c \sim 1$ and no appreciable development of fingers is observed. The order-of-magnitude increase in λ_c at the same displacement parameters in comparison with experiments in which the displacing liquid does not wet the porous medium was caused mainly by an order-of-magnitude increase in Φ_c for the given type of displacement. The change in Φ_c, which characterizes the integrated action of the capillary forces on the displacement front, occurs because of the different shape of the curves of the relative phase permeabilities and the capillary pressure during draining and soaking of the same porous medium [5]. Computational modeling of finger development using a model with a large width ($H' > 10H$ and $H'/\lambda > 10$) showed that, in this case, finger development occurs qualitatively, as in Figs. 1-4. The value of λ_c cannot increase substantially as a result of an increase in velocity in the given experiments since at $v_0 > 10^{-4}$ m/sec the capillary number $N_c = v_0\mu/\sigma > 10^{-5}$ and the displacement becomes a nonequilibrium process.

Comparison of the results of the experiments and computations showed that when the porous medium is wetted well by one of the liquids the viscous fingering is described well in the Masket–Leverett model. In this case, capillary return flows of liquid from the head part to the tail part of the fingers are the main mechanism regulating the development of fingers during the nonlinear stage of their growth.

LITERATURE CITED

1. R. M. Kats and V. B. Taranchuk, "Review of papers on the study of the stability of filtration flows," in: Dynamics of Multiphase Media [in Russian], Inst. Teor. Prikl. Mekh., Sib. Otd., Akad. Nauk SSSR, Novosibirsk (1981).
2. G. M. Homsy, "Viscous fingering in porous media," Ann. Rev. Fluid Mech., 19, 271 (1987).
3. R. L. Chuoke, P. Van Meurs, and C. Van der Poel, "The instability of slow, immiscible, viscous liquid-liquid displacement in permeable media," Trans. AIME, 216, 188 (1959).
4. D. Bensimon, L. P. Kadanoff, et al., "Viscous flow in two dimensions," Rev. Mod. Phys., 58, No. 4 (1986).
5. G. I. Barenblatt, V. M. Entov, and V. M. Ryzhik, Motion of Liquids and Gases in Natural Strata [in Russian], Nedra, Moscow (1984).
6. V. M. Ryzhik and B. E. Kisilenko, "Study of the movement of the oil–water interface in a porous medium," in: Physicogeological Factors in the Development of Oil and Oil–Gas Condensate Fields [in Russian], Nedra, Moscow (1969).
7. O. B. Bocharov and V. V. Kuznetsov, "Computational modeling of unstable displacement in a porous medium," in: Numerical Methods of Solving Filtration Problems of a Multiphase Incompressible Liquid [in Russian], Inst. Teor. Prikl. Mekh., Sib. Otd., Akad. Nauk SSSR, Novosibirsk (1987).